

Diffractive ρ production at small x in future Electron - Ion Colliders

V. P. Gonçalves^{1,2}, F. S. Navarra³ and D. Spiering³

¹ *Department of Astronomy and Theoretical Physics, Lund University, 223-62 Lund, Sweden.*

² *Instituto de Física e Matemática, Universidade Federal de Pelotas,
Caixa Postal 354, CEP 96010-900, Pelotas, RS, Brazil and*

³ *Instituto de Física, Universidade de São Paulo, CEP 05315-970 São Paulo, SP, Brazil.*

The future Electron - Ion (eA) Collider is expected to probe the high energy regime of the QCD dynamics, with the exclusive vector meson production cross section being one of the most promising observables. In this paper we complement previous studies of exclusive processes presenting a comprehensive analysis of diffractive ρ production at small x . We compute the coherent and incoherent cross sections taking into account non-linear QCD dynamical effects and considering different models for the dipole - proton scattering amplitude and for the vector meson wave function. The dependence of these cross sections with the energy, photon virtuality, nuclear mass number and squared momentum transfer is analysed in detail. Moreover, we compare the non-linear predictions with those obtained in the linear regime. Finally, we also estimate the exclusive photon, J/Ψ and ϕ production and compare with the results obtained for ρ production. Our results demonstrate that the analysis of diffractive ρ production in future electron - ion colliders will be important to understand the non-linear QCD dynamics.

PACS numbers: 12.38.-t, 13.60.Hb, 24.85.+p

I. INTRODUCTION

One of the main goals of the future Electron - Ion Colliders (EIC) [1–4] is the study of the hadronic structure in the non-linear regime of the Quantum Chromodynamics (QCD). Theoretically, the magnitude of the non-linear effects is expected to be amplified by the nuclear medium, which should allow us to determine the presence of gluon saturation effects, their magnitude and which is the correct theoretical framework for their description (For reviews see, e.g., Ref. [5]). During the last years many authors have proposed the study of several inclusive and diffractive observables [6–22] in order to search for non-linear effects in eA collisions. One of the most promising observables is the exclusive production of vector mesons or photons, which are experimentally clean and can be unambiguously identified by the presence of a rapidity gap in the final state. As these processes are driven by the gluon content of the target, with the cross sections being proportional to the square of the scattering amplitude, they are strongly sensitive to the underlying QCD dynamics. The diffractive production of J/Ψ and ϕ in eA processes was analysed in detail in Refs. [14, 16–19] taking into account non-linear effects, and predictions for the energy, virtuality and transverse momentum dependencies were presented. In contrast, in the case of ρ production, only predictions for the energy and virtuality dependencies were presented in Refs. [14, 17]. Our goal in this paper is to complement and extend these previous studies and present a comprehensive analysis of ρ production. We present, for the first time, predictions for the squared momentum transfer (t) distributions, which are an important source of information about the spatial distribution of the gluons in a nucleus and about fluctuations of the nuclear color fields. We take into account non-linear QCD effects and consider different models for the dipole - proton scattering amplitude as well as for the vector meson wave function. Moreover, we present a comparison between the non-linear predictions with those obtained using a linear model for the QCD dynamics. Finally, we present a comparison between our predictions for the ρ and those for the exclusive photon, J/Ψ and ϕ production.

This paper is organized as follows. In the next Section we present a brief review of the description of diffractive ρ production in the color dipole formalism. In Section III we present our results for the energy, virtuality and momentum transfer dependencies of the ρ cross section. A comparison between our predictions for the ρ production with those for other final states and the impact of the non-linear effects in the t - distributions is investigated. Finally, in Section IV we summarize our main conclusions.

II. DIFFRACTIVE ρ PRODUCTION IN THE COLOR DIPOLE PICTURE

In the color dipole picture, the $eA \rightarrow e\rho Y$ process can be factorized in terms of the fluctuation of the virtual photon into a $q\bar{q}$ color dipole, the dipole-nucleus scattering by a color singlet exchange and the recombination into the exclusive final state ρ . The final state is characterized by the presence of a rapidity gap. The dipole - nucleus interactions can be classified as coherent or incoherent. If the nucleus scatters elastically, $Y = A$, the process is called coherent production and can be represented by the diagram in Fig. 1 (left panel). On the other hand, if

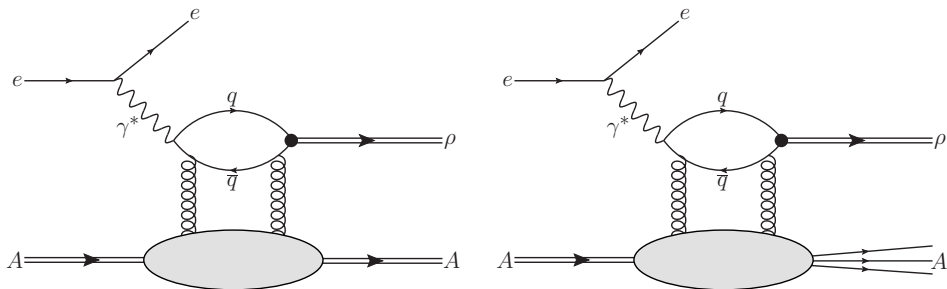


FIG. 1: Diffractive ρ production in coherent (left panel) and incoherent (right panel) eA collisions.

the nucleus scatters inelastically, i.e. breaks up ($Y = A'$), the process is denoted incoherent production and can be represented as in Fig. 1 (right panel). As discussed e.g. in Refs. [16, 18, 19], these different processes probe distinct properties of the gluon density of the nucleus. While coherent processes probe the average spatial distribution of gluons, the incoherent ones are determined by fluctuations and correlations in the gluon density. In order to access these informations, it is fundamental to understand the contribution of each process in distinct kinematical regimes. One of our main motivations is to study the energy, virtuality and transverse momentum dependencies of the ρ cross section. Another one, is the fact that the study of the ρ production at different photon virtualities allows to probe the transition between the non-linear and linear regimes of the QCD dynamics. While at large - Q^2 the process is dominated by small size dipoles, where the contribution of non-linear effects is negligible, at small photon virtualities the main contribution comes from large size dipoles, with the dynamics being determined by the gluon saturation effects. In contrast, J/Ψ production is dominated by small dipoles, which implies a smaller contribution of non-linear effects. Therefore, the study of ρ production in coherent and incoherent processes is ideal to investigate in detail the impact of the saturation effects in the spatial distribution, fluctuations and correlations in the nuclear gluon density.

A. ep collisions

Let us start our analysis presenting a brief review of the description of the diffractive ρ production in ep collisions at high energies. The $\gamma^*p \rightarrow \rho p$ cross section can be written as

$$\sigma(\gamma^*p \rightarrow \rho p) = \int_{-\infty}^0 \frac{d\sigma}{dt} dt = \frac{1}{16\pi} \sum_{i=T,L} \int_{-\infty}^0 |\mathcal{A}_i^{\gamma^*p \rightarrow \rho p}(x, Q^2, \Delta)|^2 dt, \quad (1)$$

with the amplitude for producing an exclusive ρ meson diffractively in an electron - proton scattering being given by

$$\mathcal{A}_{T,L}^{\gamma^*p \rightarrow \rho p}(x, Q^2, \Delta) = i \int dz d^2\mathbf{r} d^2\mathbf{b}_p e^{-i[\mathbf{b}_p - (1-z)\mathbf{r}] \cdot \Delta} (\Psi^{\rho^*}\Psi)_{T,L} 2\mathcal{N}^p(x, \mathbf{r}, \mathbf{b}_p) \quad (2)$$

where T and L denotes the transverse and longitudinal polarizations of the virtual photon, $(\Psi^{\rho^*}\Psi)_i$ denotes the wave function overlap between the virtual photon and ρ meson wave functions, $\Delta = -\sqrt{t}$ is the momentum transfer and \mathbf{b}_p is the impact parameter of the dipole relative to the proton. Moreover, the variables \mathbf{r} and z are the dipole transverse radius and the momentum fraction of the photon carried by a quark (an antiquark carries then $1 - z$), respectively. $\mathcal{N}^p(x, \mathbf{r}, \mathbf{b}_p)$ is the forward dipole-proton scattering amplitude (for a dipole at impact parameter \mathbf{b}_p) which encodes all the information about the hadronic scattering, and thus about the non-linear and quantum effects in the hadron wave function. It depends on the γ - hadron center - of - mass reaction energy, W , through the variable:

$$x = \frac{Q^2 + m_V^2}{Q^2 + W^2} \quad (3)$$

where Q^2 and m_V are the photon virtuality and vector meson mass, respectively. Consequently, the cross section for ρ production at low Q^2 is much more sensitive to low x effects than the one for production of heavy mesons.

At high energies the evolution with the rapidity $Y = \ln \frac{1}{x}$ of $\mathcal{N}^p(x, \mathbf{r}, \mathbf{b}_p)$ is given in the Color Glass Condensate (CGC) formalism [23] by the infinite hierarchy of equations, the so called Balitsky-JIMWLK equations [23, 24], which reduces in the mean field approximation to the Balitsky-Kovchegov (BK) equation [24, 25]. This equation has been solved in Ref. [26] taking into account the running coupling corrections and assuming the translational invariance

approximation, which implies $\mathcal{N}^p(x, \mathbf{r}, \mathbf{b}_p) = \mathcal{N}^p(x, \mathbf{r})S(\mathbf{b}_p)$. As a consequence, the dipole - proton cross section, defined by

$$\sigma_{dp}(x, \mathbf{r}) = 2 \int d^2 \mathbf{b}_p \mathcal{N}^p(x, \mathbf{r}, \mathbf{b}_p), \quad (4)$$

will be given by $\sigma_{dp}(x, \mathbf{r}) = \sigma_0 \cdot \mathcal{N}^p(x, \mathbf{r})$, with the normalization of the dipole cross section (σ_0) being fitted to data. Hereafter we will denote by rcBK the predictions obtained using the numerical solution of running coupling BK equation for $\mathcal{N}^p(x, \mathbf{r})$ obtained in Ref. [26]. Moreover, we will also consider the bCGC model, which is based on the CGC formalism and takes into account the impact parameter dependence of the dipole - proton scattering amplitude. In this model the dipole - proton scattering amplitude is given by [27]

$$\mathcal{N}^p(x, \mathbf{r}, \mathbf{b}_p) = \begin{cases} \mathcal{N}_0 \left(\frac{r Q_s(b_p)}{2} \right)^{2 \left(\gamma_s + \frac{\ln(2/r Q_s(b_p))}{\kappa \lambda Y} \right)} & r Q_s(b_p) \leq 2 \\ 1 - e^{-A \ln^2(B r Q_s(b_p))} & r Q_s(b_p) > 2 \end{cases} \quad (5)$$

with $\kappa = \chi''(\gamma_s)/\chi'(\gamma_s)$, where χ is the LO BFKL characteristic function. The coefficients A and B are determined uniquely from the condition that $\mathcal{N}^p(x, \mathbf{r}, \mathbf{b}_p)$, and its derivative with respect to $r Q_s(b_p)$, are continuous at $r Q_s(b_p) = 2$. The impact parameter dependence of the proton saturation scale $Q_s(b_p)$ is given by:

$$Q_s(b_p) \equiv Q_s(x, b_p) = \left(\frac{x_0}{x} \right)^{\frac{\lambda}{2}} \left[\exp \left(-\frac{b_p^2}{2 B_{CGC}} \right) \right]^{\frac{1}{2\gamma_s}}, \quad (6)$$

with the parameter B_{CGC} being obtained by a fit of the t -dependence of exclusive J/ψ photoproduction. Moreover, the factors \mathcal{N}_0 and γ_s were taken to be free. In what follows we consider the set of parameter obtained in Ref. [34] by fitting the recent HERA data for the reduced ep cross sections: $\gamma_s = 0.6599$, $\kappa = 9.9$, $B_{CGC} = 5.5 \text{ GeV}^{-2}$, $\mathcal{N}_0 = 0.3358$, $x_0 = 0.00105$ and $\lambda = 0.2063$. In our calculations we will consider the rcBK and bCGC models in order to estimate the dependence of our predictions on the model used to describe the dipole - proton amplitude. It is important to emphasize that both models predict the saturation of \mathcal{N}^p at large dipole sizes and that the non-linear effects become negligible at small - \mathbf{r} . However, these models predict a different behavior in the transition region between small and large dipoles, as well as distinct energy dependence for the saturation scale.

The precise form of the wave function overlap $(\Psi^{\rho*} \Psi)_i$ in Eq. [2] is still an open question. In contrast to the photon wave function, which is well known in the literature (See e.g. [27]), the ρ wave function is still a subject of investigation. The simplest approach is to assume that the ρ is predominantly a quark-antiquark state and that the spin and polarization structure is the same as in the photon [28–31] (for other approaches see, for example, Ref. [32]). As a consequence, the wave function overlap is given by (For details see Ref. [27])

$$(\Psi_V^* \Psi)_T = \frac{\hat{e}_f e}{4\pi} \frac{N_c}{\pi z(1-z)} \left\{ m_f^2 K_0(\epsilon r) \phi_T(r, z) - [z^2 + (1-z)^2] \epsilon K_1(\epsilon r) \partial_r \phi_T(r, z) \right\}, \quad (7)$$

$$(\Psi_V^* \Psi)_L = \frac{\hat{e}_f e}{4\pi} \frac{N_c}{\pi} 2Qz(1-z) K_0(\epsilon r) \left[M_V \phi_L(r, z) + \delta \frac{m_f^2 - \nabla_r^2}{M_V z(1-z)} \phi_L(r, z) \right], \quad (8)$$

where \hat{e}_f is the effective charge of the vector meson, m_f is the quark mass, $N_c = 3$, $\epsilon^2 = z(1-z)Q^2 + m_f^2$ and $\phi_i(r, z)$ define the scalar part of the vector meson wave functions. In order to estimate the dependence of our predictions on the model for the ρ wave function, in what follows we will consider the Boosted Gaussian ($\delta = 1$) and Gaus-LC ($\delta = 0$) models for $\phi_T(r, z)$ and $\phi_L(r, z)$, which are largely used in the literature. In the Boosted Gaussian model the functions $\phi_i(r, z)$ are given by [27]

$$\phi_{T,L}(r, z) = N_{T,L} z(1-z) \exp \left[-\frac{m_f^2 R^2}{8z(1-z)} - \frac{2z(1-z)r^2}{R^2} + \frac{m_f^2 R^2}{2} \right]. \quad (9)$$

In contrast, in the Gaus-LC model, they are given by [27]

$$\phi_T(r, z) = N_T [z(1-z)]^2 \exp(-r^2/2R_T^2), \quad (10)$$

$$\phi_L(r, z) = N_L z(1-z) \exp(-r^2/2R_L^2). \quad (11)$$

The parameters N_i , R and R_i are determined by the normalization condition of the wave function and by the decay width. In Table I we present the value of these parameters for the ρ wave function. As demonstrated in Ref. [27], the dipole size dependence of the overlap functions are very similar for the longitudinal polarization. On the other hand,

Model	M_ρ/GeV	m_f/GeV	N_T	R_T^2/GeV^{-2}	R^2/GeV^{-2}	N_L	R_L^2/GeV^{-2}
Gaus-LC	0.776	0.14	4.47	21.9	–	1.79	10.4
Boosted Gaussian	0.776	0.14	0.911	–	12.9	0.853	–

TABLE I: Parameters of the Gaus-LC and Boosted Gaussian models for the ρ wave function.

in the case of transverse photons, the predictions differ at small values of Q^2 . The impact of using different models in the ep cross section is small, with the predictions being compatible with HERA data within the experimental errors (See e.g. Refs. [27, 33, 34]). Similar conclusions have been obtained in the analysis of the vector meson production in ultraperipheral collisions performed in Ref. [35]. However, the impact on the coherent and incoherent eA cross sections is still an open question, which should be quantified in order to obtain realistic predictions. This is one of the main motivations to present the Boosted Gaussian and Gauss - LC predictions in the next section.

B. eA collisions

Let us discuss now diffractive ρ production in eA collisions. In this case we must consider separately the coherent and incoherent processes. In the coherent case, the nucleus is required to remain in its ground state, i.e. intact after the interaction. It corresponds to take the average over the nuclear wave function at the level of the scattering amplitude. In other words, the coherent cross section is obtained by averaging the amplitude before squaring it. Consequently, the differential distribution (with respect to the squared momentum transfer t) for coherent interactions will be given by

$$\frac{d\sigma_{coh}}{dt} = \frac{1}{16\pi} \left| \langle \mathcal{A}^{\gamma^* A \rightarrow \rho A}(x, Q^2, \Delta_A) \rangle \right|^2, \quad (12)$$

where

$$\langle \mathcal{A}^{\gamma^* A \rightarrow \rho A}(x, Q^2, \Delta_A) \rangle = i \int d^2\mathbf{b}_A \int dz d^2\mathbf{r} e^{-i\mathbf{b}_A \cdot \Delta_A} (\Psi^{\rho^*} \Psi)_{T,L} 2\mathcal{N}^A(x, \mathbf{r}, \mathbf{b}_A), \quad (13)$$

with $\Delta_A^2 = -t$ and \mathbf{b}_A being the impact parameter between the dipole and the nucleus. At large nuclei, the forward dipole-nucleus amplitude can be expressed as follows

$$\mathcal{N}^A(x, \mathbf{r}, \mathbf{b}_A) = 1 - \exp \left[-\frac{1}{2} \sigma_{dp}(x, \mathbf{r}^2) A T_A(\mathbf{b}_A) \right], \quad (14)$$

where σ_{dp} is the dipole-proton cross section and $T_A(\mathbf{b}_A)$ is the nuclear profile function, which is obtained from a 3-parameter Fermi distribution for the nuclear density normalized to 1. The above expression can be derived considering the Glauber-Gribov formalism [36], and it takes into account the multiple elastic rescattering diagrams of the $q\bar{q}$ pair. It is justified in the large coherence length regime ($l_c \gg R_A$), where the transverse separation \mathbf{r} of partons in the multiparton Fock state of the photon becomes a conserved quantity, i.e. the size of the pair \mathbf{r} becomes eigenvalue of the scattering matrix. It is important to emphasize that this model for \mathcal{N}^A allows to describe the current experimental data on the nuclear structure function [12, 13, 37] and it has been used in previous studies [14, 17, 22] to estimate inclusive and exclusive eA observables. The corresponding integrated cross section will be given by [14, 38]

$$\sigma^{coh}(\gamma^* A \rightarrow \rho A) = \int d^2\mathbf{b}_A \left| \int d^2\mathbf{r} \int dz \Psi_\rho^*(\mathbf{r}, z) \mathcal{N}^A(x, \mathbf{r}, \mathbf{b}_A) \Psi_{\gamma^*}(\mathbf{r}, z, Q^2) \right|^2. \quad (15)$$

On the other hand, if the average over the nucleon positions is at the cross section level, the nucleus can break up and the resulting incoherent cross section will be proportional to the variance of the amplitude with respect to the nucleon configurations of the nucleus, i.e., it will measure the fluctuations of the gluon density inside the nucleus (For a detailed derivation see e.g. Refs. [18, 19]). The integrated cross section for incoherent processes can be expressed as [14, 38]

$$\sigma^{inc}(\gamma^* A \rightarrow \rho A) = \frac{|\mathcal{I}m \mathcal{A}(s, t=0)|^2}{16\pi B} \quad (16)$$

where at high energies ($l_c \gg R_A$) [38]:

$$|\mathcal{I}m \mathcal{A}|^2 = \int d^2\mathbf{b}_A A T_A(\mathbf{b}_A) \left| \int d^2\mathbf{r} \int dz \Psi_\rho^*(\mathbf{r}, z) \left[\sigma_{dp} \exp \left(-\frac{1}{2} \sigma_{dp} A T_A(\mathbf{b}_A) \right) \right] \Psi_{\gamma^*}(\mathbf{r}, z, Q^2) \right|^2 \quad (17)$$

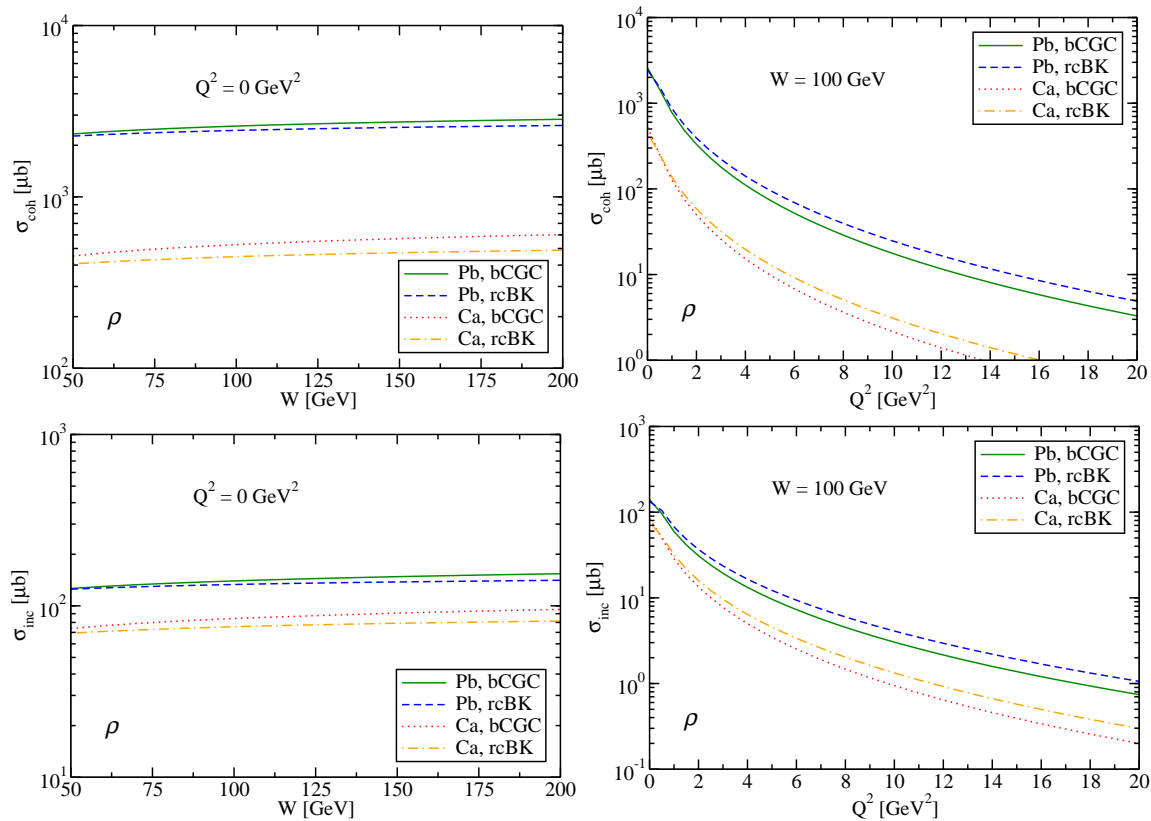


FIG. 2: (Color online) Energy and virtuality dependencies of the coherent (upper panels) and incoherent (lower panels) cross sections for two different nuclei. Predictions obtained using the Gauss-LC model for the ρ wave function.

with the t slope (B) being the same as in the case of a nucleon target. In the incoherent case, the $q\bar{q}$ pair attenuates with a constant absorption cross section, as in the Glauber model, except that the whole exponential is averaged rather than just the cross section in the exponent. For the calculation of the differential cross section $d\sigma/dt$ for incoherent interactions we apply for the ρ production the treatment presented in Ref. [18], which is valid for $t \neq 0$. Consequently, we have that

$$\frac{d\sigma_{inc}}{dt} = \frac{1}{16\pi} \sum_{i=T,L} \int dz dz' d^2\mathbf{r} d^2\mathbf{r}' (\Psi^{\rho*}\Psi)_i(z, \mathbf{r}, Q^2) (\Psi^{\rho*}\Psi)_i(z', \mathbf{r}', Q^2) \langle |\mathcal{A}|^2 \rangle, \quad (18)$$

with the average of the squared scattering amplitude being approximated by [18]

$$\begin{aligned} \langle |\mathcal{A}(\mathbf{r}, \mathbf{r}', t)|^2 \rangle &= 16\pi^2 B_p^2 \int d^2\mathbf{b} e^{-B_p \Delta_A^2} \mathcal{N}^p(x, \mathbf{r}) \mathcal{N}^p(x, \mathbf{r}') A T_A(\mathbf{b}_A) \\ &\times \exp \left\{ -2\pi(A-1) B_p T_A(\mathbf{b}_A) [\mathcal{N}^p(x, \mathbf{r}) + \mathcal{N}^p(x, \mathbf{r}')] \right\}, \end{aligned} \quad (19)$$

where $\mathcal{N}^p(x, \mathbf{r})$ is the dipole - proton scattering amplitude. The parameter B_p is associated to the impact parameter profile function in the proton and can be determined by the normalization σ_0 of the dipole - proton cross section, since $B_p = \sigma_0/4\pi$.

III. RESULTS

In what follows we will present our predictions for the coherent and incoherent ρ production considering different models for the dipole - proton scattering amplitude and for the ρ wave function. Our main focus will be in the kinematical region of small values of the Bjorken - x variable that will be probed in the future electron - ion collider facility to be constructed in the USA [3]. Basically, we will restrict our analysis to small virtualities ($Q^2 \leq 10 \text{ GeV}^2$)

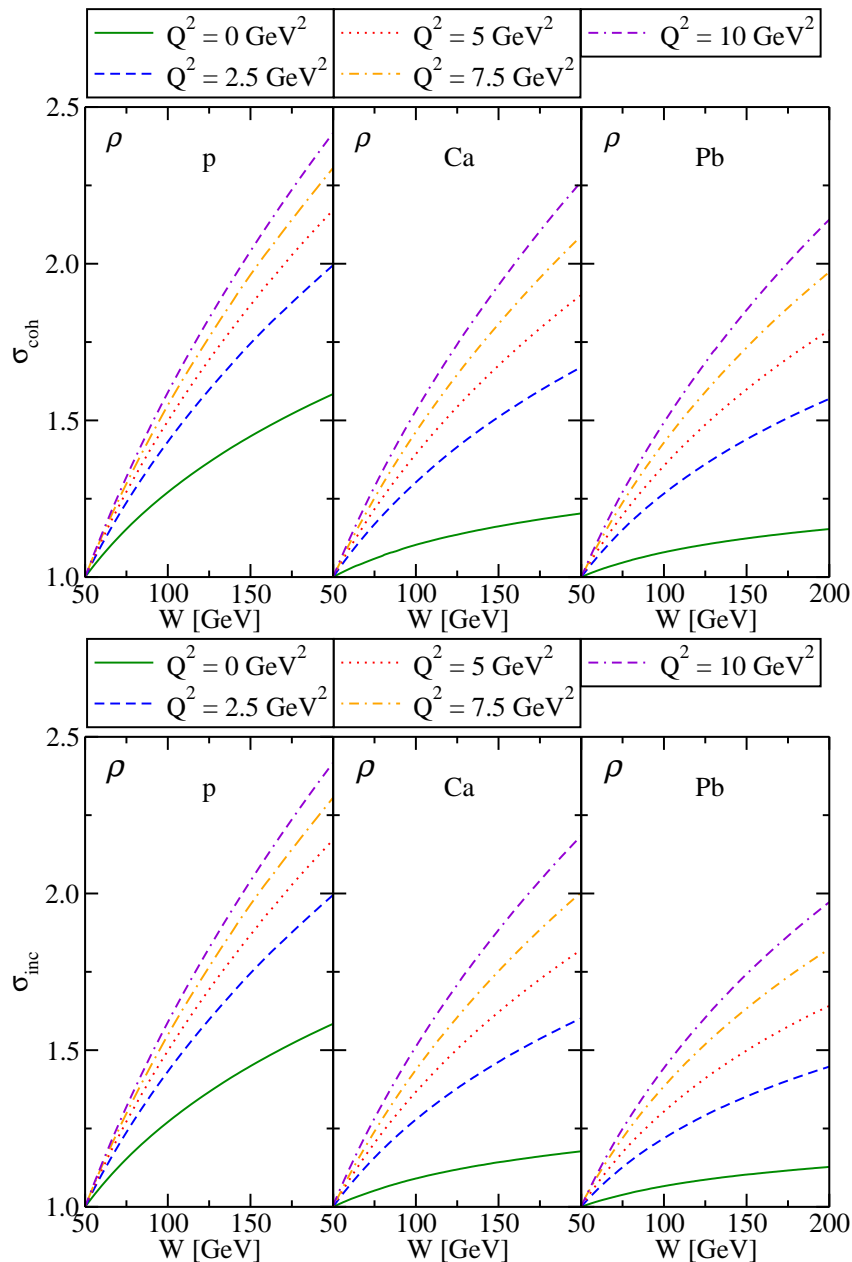


FIG. 3: (Color online) Energy dependence of the normalized coherent (upper panels) and incoherent (lower panels) cross sections for different photon virtualities Q^2 . The results for the ρ production in ep collisions are presented for comparison. Predictions obtained using the Gaus-LC model for the ρ wave function and the bCGC model for the dipole - proton scattering amplitude.

and center - of - mass energies W of the order of 100 GeV. However, it is important to emphasize that the magnitude of the non-linear effects increases with the energy, which implies that our main conclusions should also be valid for the diffractive ρ production in eA collisions at the LHeC [4].

Initially let us address the energy W and virtuality Q^2 dependencies of the coherent and incoherent cross sections considering two different nuclei, $A = 40$ (Ca) and 208 (Pb), and the Gaus-LC model for the overlap function. Moreover, two distinct models for the dipole - proton scattering amplitude are used to estimate the cross sections. In the left panels of the Fig. 2 we present the energy dependence of our predictions assuming $Q^2 = 0$. We observe that the cross sections increase with the energy and nuclear mass number. The coherent processes have a stronger A dependence in comparison to the incoherent one, which implies that the dominance of the coherence processes increases with the

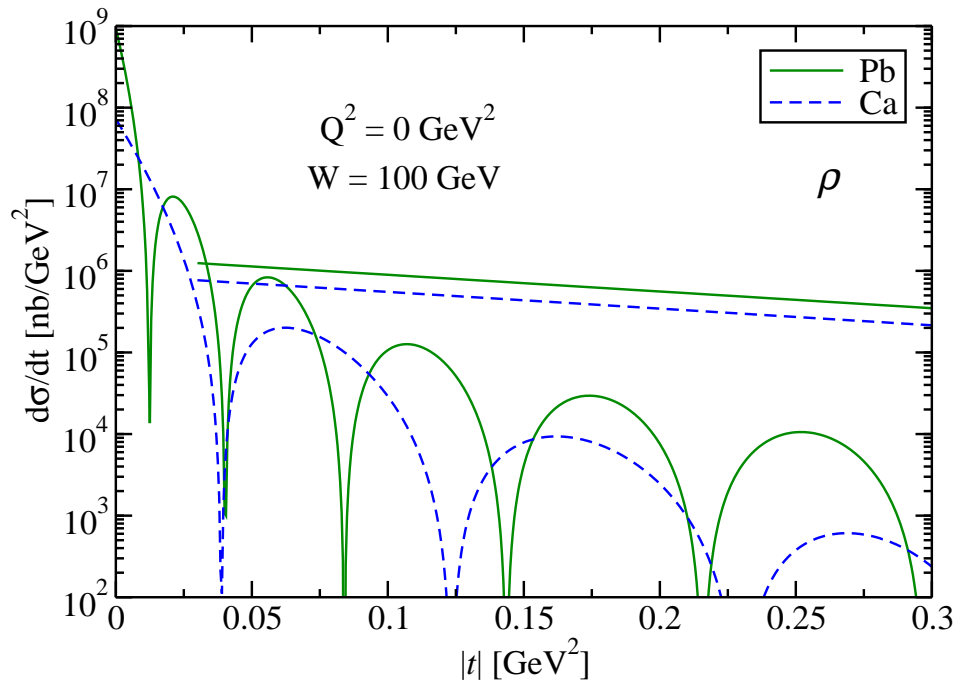


FIG. 4: (Color online) Differential cross section for coherent and incoherent interactions for different nuclei. Predictions obtained using the Gaus-LC model for the ρ wave function and the bCGC model for the dipole - proton scattering amplitude.

atomic number. Regarding the dependence on the model used for the dipole - proton scattering amplitude, we have that the bCGC and rcBK models yield very similar predictions at large nuclei. At lighter nuclei the bCGC predictions are $\approx 15\%$ larger than the rcBK one, which is directly associated to the different transition between the linear and non-linear regime predicted by these models (See, e.g. Fig. 3 in Ref. [22]). This distinct behavior has direct impact on the Q^2 dependence of the coherent and incoherent cross sections, presented in the right panels of Fig. 2. We have that the cross sections decrease with the photon virtuality, with the difference between the bCGC and rcBK predictions increasing with Q^2 . Consequently, the probe of the cross sections at intermediate Q^2 , e.g. $Q^2 = 10 \text{ GeV}^2$, can be useful to constrain the description of the dipole - proton scattering amplitude.

As discussed in the previous Section and shown by the HERA data, the diffractive ρ production probes the transition between the soft and hard QCD regimes, with the energy dependence being strongly sensitive to Q^2 . In particular, at small - Q^2 , the energy dependence of the ep cross section is similar to that expected for soft processes ($\sigma \propto W^\delta$, with $\delta \approx 0.22$), while for large Q^2 one has $\delta \approx 0.8$, compatible with the dependence expected for hard processes. In order to check how this behavior is modified by the nuclear medium, in Fig. 3 we present our predictions for the energy dependence of the coherent (upper panels) and incoherent (lower panels) cross sections considering different values of the photon virtuality. In order to facilitate the comparison, the distinct predictions for $W = 50 \text{ GeV}$ have been normalized to the unity. Moreover, for completeness, in the left panels we present the predictions for the ep cross sections. As in the proton case, the slope of the distinct curves increases with the virtuality, with the growth being smaller for heavier nuclei. Moreover, we can observe that the energy dependence is strongly modified at larger nuclei and smaller Q^2 . This behaviour is expected, since in this kinematical range the magnitude of the non-linear effects is predicted to be amplified. At large Q^2 , the difference between the slopes for different atomic mass number decreases, which is associated to the fact that the linear regime becomes dominant. Therefore, the study of the diffractive ρ production at large nuclei and small - Q^2 is ideal to probe the gluon saturation effects in the QCD dynamics.

Let us now extend our analysis to the differential distributions $d\sigma/dt$ for coherent and incoherent interactions. In the case of the incoherent predictions we only present predictions for $|t| \geq 0.03 \text{ GeV}^2$, since the model proposed in Ref. [18] and used in our calculations fails to describe the vanishing of the incoherent cross section as $|t| \rightarrow 0$. Our motivation to analyse in detail these processes is associated to the fact that the precise separation of these events will allow us to access the spatial distribution of the gluon density in the nucleus through the Fourier transform of the coherent cross section [19] as well as to study the incoherent processes which probe the fluctuations in the interaction strengths of parton configurations in the nuclear wave function with large values of the saturation scale [21]. In Fig. 4 we present our predictions for the coherent and incoherent ρ cross section for different nuclei and $Q^2 = 0$ considering

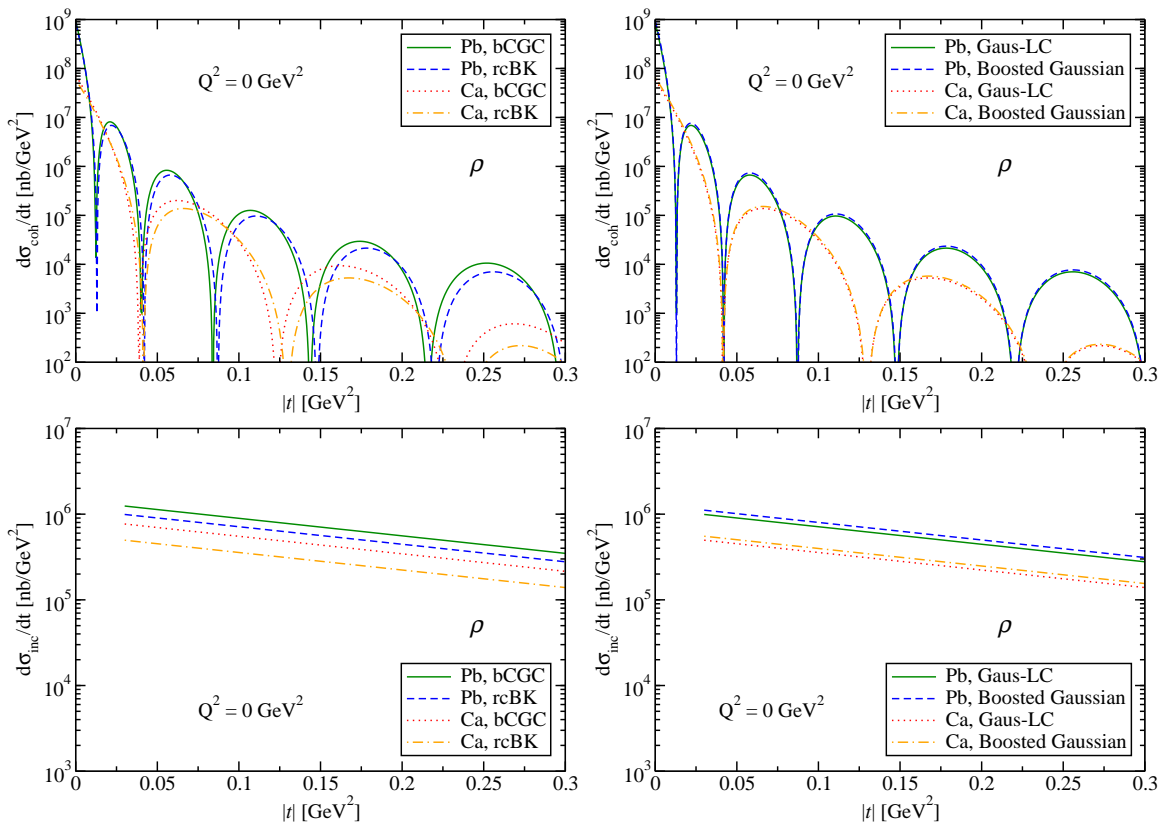


FIG. 5: (Color online) Differential cross section for coherent (upper panels) and incoherent (lower panels) interactions. Left panels: Predictions obtained considering different models for the dipole - proton scattering amplitude and the Gaus-LC model for the ρ wave function. Right panels: Predictions obtained considering different models for the ρ wave function and the bCGC model for the dipole - proton scattering amplitude.

the bCGC and Gaus-LC models for the dipole - proton amplitude and ρ wave function. We find that the coherent cross section clearly exhibits the typical diffractive pattern, with the dips in the range $|t| \leq 0.3$ GeV² increasing with the mass atomic number. Moreover, the coherent processes are characterized by a sharp forward diffraction peak and the incoherent one by a t - dependence very similar to that for the ρ production off free nucleons. The incoherent processes dominate at large - $|t|$ and the coherent ones at small values of the momentum transfer. This behaviour can be easily understood: with the increasing of the momentum kick given to the nucleus the probability that it breaks up becomes larger. As a consequence, the eA interactions at large - $|t|$ are dominated by incoherent processes. Therefore, the analysis of the t dependence can be useful to separate coherent and incoherent interactions. However, as discussed in detail in Refs. [16, 19], the experimental separation of these processes is still a challenge. An alternative is the detection of the fragments of the nuclear breakup present in the incoherent processes. e.g. the detection of emitted neutrons by zero - degree calorimeters.

In Fig. 5 we analyse the dependence of our predictions on the basic inputs of our calculations. In particular, in the left panels we present our predictions considering different models for the dipole - proton scattering amplitude and in the right panels for different wave functions. We find that the positions of the dips are almost independent of the dipole - proton model used as input in the calculations, as already observed in Ref. [22] for the nuclear DVCS. Moreover, we obtain that our results are almost independent of the model used to calculate the wave functions. This conclusion is also valid for the incoherent cross section, which is slightly dependent on the model used for $\mathcal{N}^p(x, \mathbf{r})$ for lighter nuclei.

In Fig. 6 we analyse the dependence on Q^2 of our predictions considering the bCGC and Gaus-LC models for the dipole - proton scattering and ρ wave function, respectively. Moreover, we present predictions for $A = Pb$ (left panels) and $A = Ca$ (right panels). As expected from the analysis of the total cross sections, the differential distributions decrease with the photon virtuality. Our results demonstrate that the position of the dips in the coherent cross sections are almost independent of Q^2 and that the t -dependence of the incoherent cross sections are similar for different values of the photon virtuality.

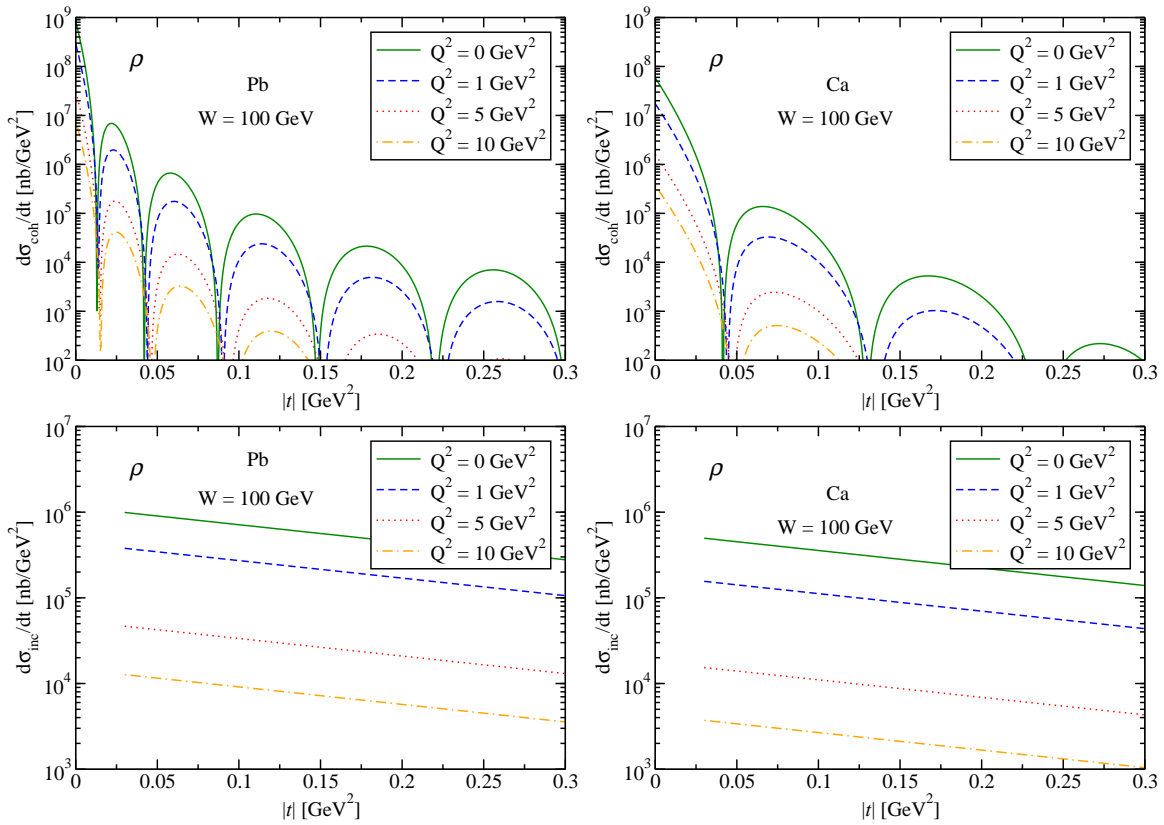


FIG. 6: (Color online) Differential cross section for coherent (upper panels) and incoherent (lower panels) interactions considering different values of Q^2 and distinct nuclei. Predictions obtained using the Gaus-LC and bCGC models.

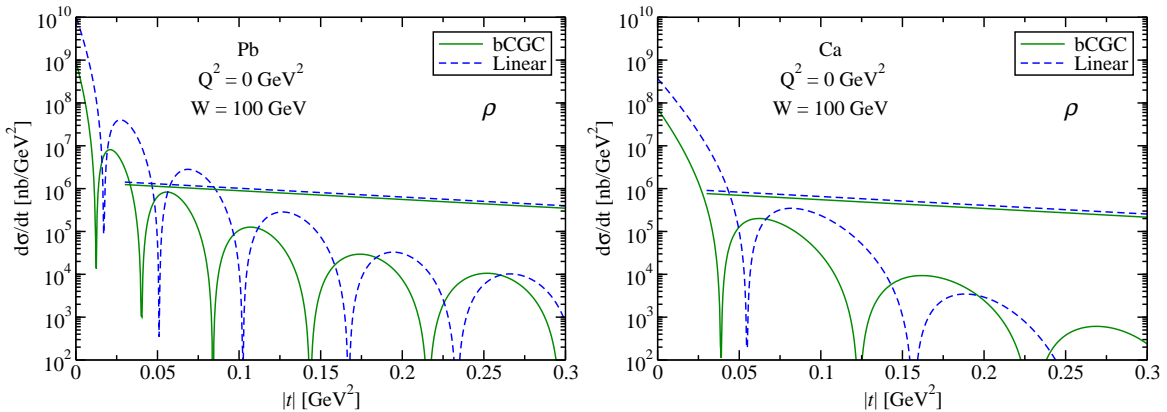


FIG. 7: (Color online) Comparison between non-linear and linear predictions for the differential cross sections in coherent and incoherent interactions. Predictions obtained using the Gaus-LC model for the ρ wave function.

One important aspect to be investigated is the impact of the non-linear effects in the diffractive ρ production. As discussed above, the coherent and incoherent cross sections are determined by the dipole - nucleus \mathcal{N}^A and dipole - proton \mathcal{N}^P scattering amplitudes, respectively. In order to estimate the magnitude of the non-linear effects, let us assume that dipole - nucleus amplitude can be expressed by

$$\mathcal{N}^A(x, r, b) = \frac{1}{2} \sigma_{dp}(x, r) AT_A(b) \quad (20)$$

with σ_{dp} expressed by Eq. (4). Moreover, we will assume in the calculation of σ_{dp} and the incoherent cross section

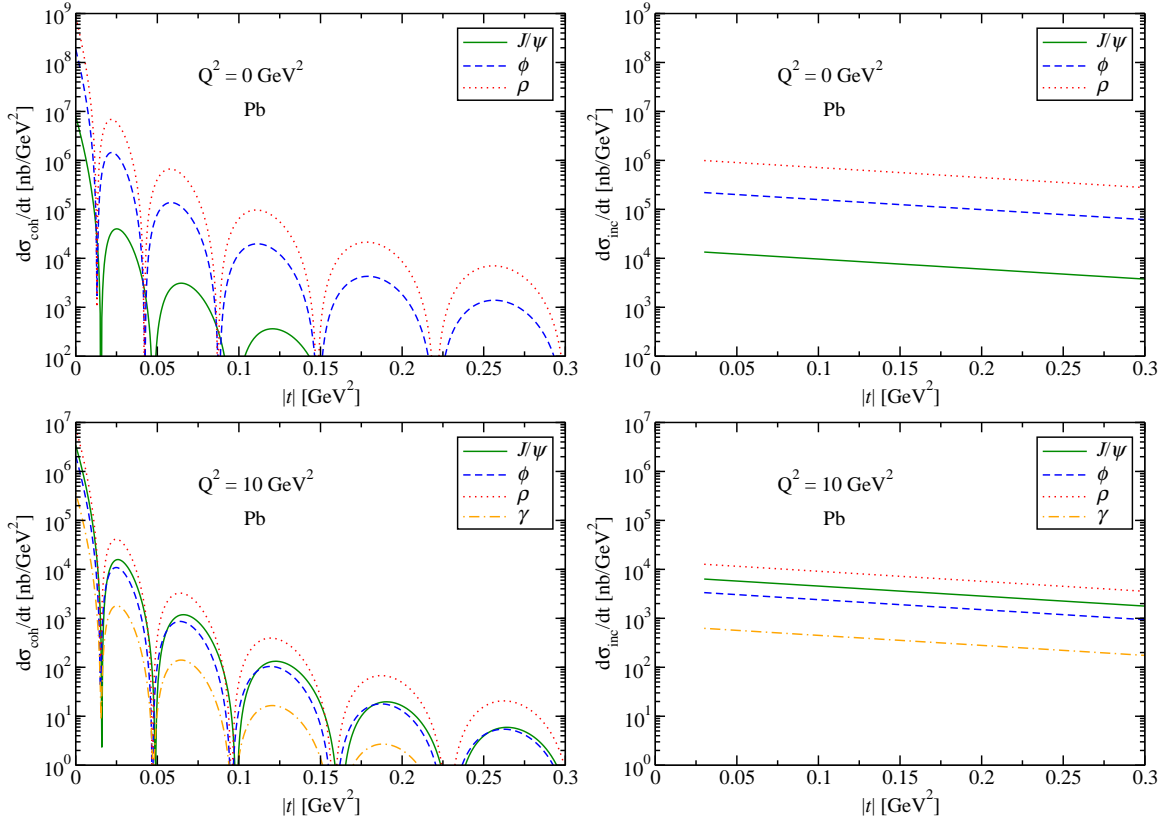


FIG. 8: (Color online) Comparison between the differential cross sections for coherent and incoherent production of different final states considering $Q^2 = 0$ (upper panels) and $Q^2 = 10 \text{ GeV}^2$ (lower panels). Predictions obtained using the Gaus-LC and bCGC models.

that $\mathcal{N}^p(x, \mathbf{r}, \mathbf{b})$ is given by the linear part of the bCGC model, which is

$$\mathcal{N}^p(x, \mathbf{r}, \mathbf{b}) = \mathcal{N}_0 \left(\frac{r Q_s(b)}{2} \right)^{2\left(\gamma_s + \frac{\ln(2/rQ_s(b))}{\kappa \lambda Y}\right)}, \quad (21)$$

with the same parameters used before in Eq. (5). The basic idea in Eq. (20) is to disregard the multiple scatterings of the dipole with the nuclei, which are taken into account the non-linear effects in the full calculation. On the other hand, Eq. (21) means that we are disregarding possible non-linear effects in the nucleon. In Fig. 7 we present a comparison between linear and non-linear predictions. We can observe that the incoherent cross sections are not strongly modified by the non-linear effects. In contrast, in the case of coherent interactions, the magnitude of the cross section and position of the dips are distinct in the non linear and linear predictions, which makes the analysis of this observable a sensitive probe of the non-linear QCD dynamics.

Finally, let us compare our predictions for the ρ production with those for other exclusive final states: J/Ψ , ϕ and γ . Our motivation to perform this comparison is associated to the fact that the lighter vector mesons (ρ and ϕ) are more sensitive to saturation effects than the J/Ψ , since the corresponding overlap functions peak at larger pair separations at a fixed photon virtuality Q^2 . Moreover, this study allows to probe the transition between the non-linear and linear regimes of the QCD dynamics by increasing the photon virtuality. In Fig. 8 we present our results for two different values of Q^2 and $A = Pb$. For $Q^2 = 0$ (upper panels) we observe that the differential cross sections decrease at heavier vector mesons and the position of the dips for the J/Ψ production is slightly different of the other mesons, which is associated to the dominance of small dipoles in this final state. In contrast, $Q^2 = 10 \text{ GeV}^2$ (lower panels), the position of the dips becomes almost identical for all exclusive final states. Therefore, the experimental analysis of heavy and light mesons at small - Q^2 can be useful to probe different regimes of the QCD dynamics.

IV. CONCLUSIONS

The study of exclusive processes in deep inelastic scattering (DIS) processes has been one of the main topics in hadronic physics during the last years. It is expected that the analysis of these processes allow us to probe the QCD dynamics at high energies, driven by the gluon content of the target (proton or nucleus) which is strongly subject to non-linear effects (parton saturation). In particular, in electron - nucleus collisions the gluon density is amplified due to the coherent contributions from many nucleons. Our goal in this paper was to extend and complement previous studies about the vector meson production in eA collisions, presenting a comprehensive analysis of the energy, virtuality, nuclear mass number and transverse momentum dependencies of the cross sections for the ρ production in the kinematical range which could be accessed in future electron - ion colliders. We have found that the energy dependence of the differential cross sections are strongly modified with the increasing of the nuclear mass number and that coherent cross section dominates at small t and the incoherent one dominates at large values of t . Our results demonstrated that the number of dips at small t increases with the atomic number, with the position of the dips being almost independent of the model used to treat the dipole - proton interaction. Moreover, we show that our predictions are insensitive to the model used to treat the ρ wave function. A comparison with other exclusive final states was presented and we have demonstrated that the non-linear effects change the positions of the dips with respect to the linear regime. These results are robust predictions of the saturation physics, which can be used to investigate non-linear QCD dynamics in the kinematical range of future electron - ion experiments.

Acknowledgments

VPG would like to thank S. Klein and H. Mantysaari by useful discussions about incoherent processes. This work was partially financed by the Brazilian funding agencies CNPq, CAPES and FAPERGS.

-
- [1] A. Deshpande, R. Milner, R. Venugopalan and W. Vogelsang, *Ann. Rev. Nucl. Part. Sci.* **55**, 165 (2005).
 - [2] D. Boer, M. Diehl, R. Milner, R. Venugopalan, W. Vogelsang, D. Kaplan, H. Montgomery and S. Vignor *et al.*, arXiv:1108.1713 [nucl-th].
 - [3] A. Accardi, J. L. Albacete, M. Anselmino, N. Armesto, E. C. Aschenauer, A. Bacchetta, D. Boer and W. Brooks *et al.*, arXiv:1212.1701 [nucl-ex].
 - [4] J. L. Abelleira Fernandez *et al.* [LHeC Study Group Collaboration], *J. Phys. G* **39**, 075001 (2012)
 - [5] F. Gelis, E. Iancu, J. Jalilian-Marian and R. Venugopalan, *Ann. Rev. Nucl. Part. Sci.* **60**, 463 (2010); E. Iancu and R. Venugopalan, arXiv:hep-ph/0303204; H. Weigert, *Prog. Part. Nucl. Phys.* **55**, 461 (2005); J. Jalilian-Marian and Y. V. Kovchegov, *Prog. Part. Nucl. Phys.* **56**, 104 (2006); J. L. Albacete and C. Marquet, *Prog. Part. Nucl. Phys.* **76**, 1 (2014).
 - [6] V. P. Goncalves, *Phys. Lett. B* **495**, 303 (2000)
 - [7] M. S. Kugeratski, V. P. Goncalves and F. S. Navarra, *Eur. Phys. J. C* **46**, 465 (2006)
 - [8] M. S. Kugeratski, V. P. Goncalves and F. S. Navarra, *Eur. Phys. J. C* **46**, 413 (2006)
 - [9] N. N. Nikolaev, W. Schafer, B. G. Zakharov and V. R. Zoller, *JETP Lett.* **84**, 537 (2007)
 - [10] H. Kowalski, T. Lappi and R. Venugopalan, *Phys. Rev. Lett.* **100**, 022303 (2008)
 - [11] H. Kowalski, T. Lappi, C. Marquet and R. Venugopalan, *Phys. Rev. C* **78**, 045201 (2008)
 - [12] E. R. Cazaroto, F. Carvalho, V. P. Goncalves and F. S. Navarra, *Phys. Lett. B* **669**, 331 (2008)
 - [13] E. R. Cazaroto, F. Carvalho, V. P. Goncalves and F. S. Navarra, *Phys. Lett. B* **671**, 233 (2009)
 - [14] V. P. Goncalves, M. S. Kugeratski, M. V. T. Machado and F. S. Navarra, *Phys. Rev. C* **80**, 025202 (2009).
 - [15] V. P. Goncalves, M. S. Kugeratski and F. S. Navarra, *Phys. Rev. C* **81**, 065209 (2010)
 - [16] A. Caldwell and H. Kowalski, *Phys. Rev. C* **81**, 025203 (2010).
 - [17] E. R. Cazaroto, F. Carvalho, V. P. Goncalves, M. S. Kugeratski and F. S. Navarra, *Phys. Lett. B* **696**, 473 (2011)
 - [18] T. Lappi and H. Mantysaari, *Phys. Rev. C* **83**, 065202 (2011)
 - [19] T. Toll and T. Ullrich, *Phys. Rev. C* **87**, 024913 (2013)
 - [20] J. T. Amaral, V. P. Goncalves and M. S. Kugeratski, *Nucl. Phys. A* **930**, 104 (2014)
 - [21] T. Lappi, H. Mantysaari and R. Venugopalan, *Phys. Rev. Lett.* **114**, 082301 (2015)
 - [22] V. P. Goncalves and D. S. Pires, *Phys. Rev. C* **91**, 055207 (2015)
 - [23] J. Jalilian-Marian, A. Kovner, L. McLerran and H. Weigert, *Phys. Rev. D* **55**, 5414 (1997); J. Jalilian-Marian, A. Kovner and H. Weigert, *Phys. Rev. D* **59**, 014014 (1999), *ibid.* **59**, 014015 (1999), *ibid.* **59** 034007 (1999); A. Kovner, J. Guilherme Milhano and H. Weigert, *Phys. Rev. D* **62**, 114005 (2000); H. Weigert, *Nucl. Phys.* **A703**, 823 (2002); E. Iancu, A. Leonidov and L. McLerran, *Nucl. Phys.* **A692**, 583 (2001); E. Ferreira, E. Iancu, A. Leonidov and L. McLerran, *Nucl. Phys.* **A701**, 489 (2002).

- [24] I. I. Balitsky, Phys. Rev. Lett. **81**, 2024 (1998); Phys. Lett. B **518**, 235 (2001); I.I. Balitsky and A.V. Belitsky, Nucl. Phys. B **629**, 290 (2002).
- [25] Y.V. Kovchegov, Phys. Rev. D **60**, 034008 (1999); Phys. Rev. D **61** 074018 (2000).
- [26] J. L. Albacete, N. Armesto, J. G. Milhano and C. A. Salgado, Phys. Rev. **D80**, 034031 (2009).
- [27] H. Kowalski, L. Motyka and G. Watt, Phys. Rev. D **74**, 074016 (2006); G. Watt and H. Kowalski, Phys. Rev. D **78**, 014016 (2008).
- [28] H. G. Dosch, T. Gousset, G. Kulzinger and H. J. Pirner, Phys. Rev. **D55**, 2602 (1997).
- [29] J. Nemchik, N. N. Nikolaev, E. Predazzi and B. G. Zakharov, Z. Phys. C **75**, 71 (1997)
- [30] J. R. Forshaw, R. Sandapen and G. Shaw, Phys. Rev. D **69**, 094013 (2004)
- [31] H. Kowalski and D. Teaney, Phys. Rev. D **68**, 114005 (2003)
- [32] J. P. B. C. de Melo and T. Frederico, Phys. Rev. C **55**, 2043 (1997).
- [33] V. P. Goncalves, M. V. T. Machado and A. R. Meneses, Eur. Phys. J. C **68**, 133 (2010).
- [34] A. H. Rezaeian and I. Schmidt, Phys. Rev. D **88**, 074016 (2013)
- [35] V. P. Goncalves and M. V. T. Machado, Phys. Rev. C **84**, 011902 (2011); V. P. Goncalves, B. D. Moreira and F. S. Navarra, Phys. Rev. C **90**, no. 1, 015203 (2014); V. P. Goncalves, B. D. Moreira and F. S. Navarra, Phys. Lett. B **742**, 172 (2015).
- [36] V. N. Gribov, Sov. Phys. JETP **30**, 709 (1970) [Zh. Eksp. Teor. Fiz. **57**, 1306 (1969)].
- [37] N. Armesto, Eur. Phys. J. C **26**, 35 (2002).
- [38] B. Z. Kopeliovich, J. Nemchik, A. Schafer and A. V. Tarasov, Phys. Rev. C **65**, 035201 (2002).